Role of retinal pigment epithelium permeability in drug transfer between posterior eye segment and systemic blood circulation

Eva Ramsay[a,b,*], Marja Hagström[b], Kati-Sisko Vellonen[a], Susanna Boman[c], Elisa Toropainen[a], Eva M. del Amo[d], Heidi Kidron[b], Arto Urtti[a,b,e], Marika Ruponen[a]

[a] School of Pharmacy, Faculty of Health Sciences, University of Eastern Finland, FI-70211 Kuopio, Finland
[b] Drug Research Program, Division of Pharmaceutical Biosciences, Faculty of Pharmacy, University of Helsinki, P.O. Box 56, FI-00014 Helsinki, Finland
[c] Finnish Food Authority, Ruokavirasto, Kuvernöörinkatu 27, 83500 Outokumpu, Finland
[d] School of Pharmacy, University of Manchester, Manchester, United Kingdom
[e] Laboratory of Biohybrid Technologies, Institute of Chemistry, St Petersburg State University, 198504 Petergof, Russia

ARTICLE INFO

ABSTRACT

Retinal pigment epithelium (RPE) is a major part of blood-retinal barrier that affects drug elimination from the vitreous to the blood and drug distribution from blood circulation into the eye. Even though drug clearance from the vitreous has been well studied, the role of RPE in the process has not been quantified. The aim of this work was to study the role of RPE clearance (CL_{RPE}) as part of drug elimination from the vitreous and ocular drug distribution from the systemic blood circulation. We determined the bidirectional permeability of eight small molecular weight drugs and bevacizumab antibody across isolated bovine RPE-choroid. Permeability of small molecules was 10^{-6}–10^{-5} cm/s showing 13–15 fold range of outward and inward permeation, while permeability of bevacizumab was lower by 2–3 orders of magnitude. Most small molecular weight drugs showed comparable outward (vitreous-to-choroid) and inward (choroid-to-vitreous) permeability across the RPE-choroid, except ciprofloxacin and ketorolac that had an over 6 and 14-fold higher outward than inward permeability, respectively, possibly indicating active transport. Six of seven tested small molecular weight drugs had outward CL_{RPE} values that were comparable with their intravitreal clearance (CL_{IVT}) values (0.84–2.6 fold difference). On the contrary, bevacizumab had an outward CL_{RPE} that was only 3.5% of the CL_{IVT}, proving that its main route of elimination (after intravitreal injection) is not RPE permeation. Experimental values were used in pharmacokinetic simulations to assess the role of the RPE in drug transfer from the systemic blood circulation to the vitreous (CL_{BV}). We conclude that for small molecular weight drugs the RPE is an important route in drug transfer between the vitreal cavity and blood, whereas it effectively hinders the movement of bevacizumab from the vitreous to the systemic circulation.

1. Introduction

The prevalence of age-related diseases at the back of the eye, such as age-related macular degeneration (AMD), diabetic retinopathy, glaucoma and macular edema is constantly growing. The diseases with neovascular changes, such as exudative AMD are treated with anti-VEGF compounds, such as Fab-fragment ranibizumab (Lucentis®), soluble receptor aflibercept (Eylea®), and antibody bevacizumab (off-label use of Avastin®). Other potential drugs for the treatment of neovascularization include tyrosine kinase inhibitors, aptamers, and siRNA [1]. Inflammations associated with diabetic macular edema, AMD, and uveitis, are treated with corticosteroids, such as triamcinolone acetonide and dexamethasone [2]. Drug treatment of these diseases is accomplished with intravitreal administration of drug solutions, suspensions or implants. Even though intravitreal injections are invasive they are the method-of-choice in the retinal drug treatment, because topical, subconjunctival and systemic drug administrations do not provide adequate drug delivery to the retina [3].

After an intravitreal injection, the drug diffuses in the vitreous humor and distributes to the neighboring tissues. All drugs are capable of diffusing from the vitreous to the anterior chamber and then eliminate from the eye via aqueous humor outflow [4]. Additionally, the drugs may be eliminated from the vitreous posteriorly, across the blood-ocular barriers, if the compound has adequate membrane permeability based on its molecular properties (e.g. size, lipophilicity) [5]. Blood-ocular barriers include two main components: blood-aqueous

barrier (BAB) and blood-retinal barrier (BRB). The BRB consists of retinal pigment epithelium (RPE) and the endothelium of the retinal vessels, whereas the BAB is formed by the posterior iris epithelium, iridial capillaries, ciliary muscle capillaries, and nonpigmented ciliary epithelium. Inter-cellular tight-junctions are found both in the BAB and the BRB, limiting the size of the paracellular space to about 2 nm (diameter) and restricting the molecular transfer between the eye and blood circulation [3,6].

The RPE is situated between the retinal photoreceptors and choroid, and it is essential for the function of the retina, maintaining the homeostasis between the neural retina and blood circulation of the fenestrated choroidal blood vessels. Due to its large surface area, the RPE is considered to be an important route of elimination of small molecular weight drugs [3]. After crossing the neural retina and RPE, the choroid acts as an eliminating sink, because the leaky choroidal vessels have high blood flow. Small molecules may cross the RPE transcellularly and paracellularly, and they have wide range of intravitreal clearance values (0.031–1.530 ml/h) [5] that depend on the ability of the compounds to permeate across the blood ocular barriers. Due to their poor permeation of the BRB, intravitreally injected proteins and other macromolecules are mainly eliminated from the vitreous to the aqueous humor outflow, resulting in low intravitreal clearance values of 0.011–0.071 ml/h [5]. In principle, drugs may cross the RPE by passive permeation and/or active transport, depending on drug concentration, expression and localization of transporters, and affinity of drug to the transporter protein. So far, evidence suggests that passive permeability is the main mechanism of drug clearance across the BRB. Recently, the RPE transporters were quantitated [7,8], but the clinical role of RPE transporters is still unclear [9].

The knowledge of the intravitreal pharmacokinetics is important in order to develop efficient retinal drug treatments as intravitreal injections or implants [5]. Furthermore, drug permeability in the BRB is a key parameter in defining distribution of drugs from the blood circulation to the posterior eye segment [10]. A reliable quantitative structure-property relationship model (QSPR) was developed for clearance of small molecular weight drugs between vitreous and blood circulation [5]. However, intravitreal clearance values do not provide information about the routes of vitreal drug elimination. Previously, permeability of some β-blocking agents and FITC-dextrans were investigated in isolated bovine RPE-choroid [11], which demonstrated the effects of the molecular size and lipophilicity (logD$_{7.4}$) on permeability. In this study, we extended this approach to eight small molecular weight drugs and one protein drug, bevacizumab (Avastin®). To our understanding RPE permeability for such drug set (with broad lipophilicity and molecular weight range) has not been previously reported in the literature. The experimental permeability values and *in vivo* intravitreal clearance values from rabbits were used to estimate the role of the RPE as intravitreal route of drug elimination and distribution route from the systemic blood circulation.

2. Materials and methods

2.1. Drug molecules

Eight small molecular weight drugs and one protein drug were chosen for the permeability study (Table 1). The cassette mixture of the small molecular weight drugs was prepared by combining the individual stock solutions (Table 1) and diluting with a balanced salt solution BSS Plus (Alcon Laboratories, TX, USA) containing 7.14 mg/ml sodium chloride, 0.38 mg/ml potassium chloride, 0.154 mg/ml calcium chloride dihydrate, 0.2 mg/ml magnesium chloride hexahydrate, 0.42 mg/ml, dibasic sodium phosphate, 2.1 mg/ml sodium bicarbonate, 0.92 mg/ml dextrose, 0.184 mg/ml glutathione disulfide, and supplemented with 10 mM Hepes (pH 7.4). The drug concentration in the cassette mixture stock solution was either 20 or 200 µg/ml, depending on the analytical limit of quantification. The concentrations of

Table 1
Drug molecules in the permeability study.

Drug molecules	Stock solution	Manufacturer
Aztreonam	10 mg/ml in DMSO	Fluka, China
Ciprofloxacin	0.5 mg/ml in 0.1 M HCl	BioChemica, China
Fluconazole	10 mg/ml in DMSO	Sigma-Aldrich, St. Louis, MO, USA
Ganciclovir	10 mg/ml in DMSO	Sigma-Aldrich, St. Louis, MO, USA
Ketorolac Tris salt	1 mg/ml in PBS	Sigma-Aldrich, St. Louis, MO, USA
Methotrexate	1 mg/ml in DMSO	Fluka, USA
Quinidine	10 mg/ml in DMSO	Sigma-Aldrich, Steinheim, Germany
Voriconazole	10 mg/ml in DMSO	Fluka, Steinheim, Germany
Bevacizumab	Avastin® 25 mg/ml	Roche Pharma AG, Grenzach-Wyhlen, Germany

aztreonam, ganciclovir, and quinidine were 200 µg/ml, whereas the other compounds were used at concentration of 20 µg/ml.

2.2. Tissue preparation

Freshly enucleated bovine eyes (> 1 year old animals) were obtained from a local slaughterhouse and delivered to the lab in CO$_2$ Independent Medium (Gibco, Life Technologies). The eyes were first cleaned of muscle and fat tissue surrounding the eye. Then the anterior part of the eye was removed by cutting circumferentially approximately 8 mm posterior from the limbus. The vitreous was gently removed from the remaining eye cup that was cut in three parts. Medium was added on the tissues to avoid drying. The neural retina was gently removed using forceps and, thereafter, the RPE-choroid was carefully isolated from sclera using scissors and curved forceps, avoiding the area of the optic nerve.

2.3. Permeability study

The isolated RPE-choroid was placed on a plastic mesh (1 mm pore size) and further located between two ring shaped silicon adapters with a circular aperture of 0.64 cm^2. The silicon adapters with the tissue was placed in a vertical Ussing/diffusion chamber (Navicyte, Harvard Apparatus, Holliston, MA). The chamber parts in contact with the silicon adapters had been treated with vacuum grease to avoid edge leakage during the experiment. BSS Plus supplemented with 10 mM Hepes (pH 7.4) buffer was added to both sides of the chambers; 5 ml in the cassette mixture experiments and 4 ml in the bevacizumab experiments. Both sides of the chambers were attached to gas tubing, supplying the tissue with gas (5% CO$_2$, 10% O$_2$, and 85% N$_2$) at a rate of 3–4 bubbles/s. The bubbling mixed the buffer solution and maintained the pH at 7.4. The chambers were maintained at 37 °C with a heating block and circulating water bath (Grant Instruments Ltd, Cambridge, England). The chambers were equipped with electrode caps and glass barrel Ag/AgCl electrodes (NaviCyte Electrodes; Harvard Apparatus) that were connected to a voltage-current clamp (VCC MC6; Physiologic Instruments, San Diego, CA) for transepithelial electrical resistance (TER) measurements as described previously [12].

Permeability of the cassette mixture drugs was studied in outward and inward directions. The outward direction mimics vitreous-to-choroid permeation (apical to basolateral), whereas the inward permeation models choroid-to-vitreous distribution (basolateral to apical side). The bevacizumab permeability was studied only in the outward direction. The permeability experiments were initiated by replacing 500–700 µl of drug solution to the donor side (cassette mix or bevacizumab). The drug concentrations in the donor side were 20 or 200 µg/ml in the cassette mix. Bevacizumab concentration in the donor side was 4.4 mg/ml. In the cassette mix study, samples of 500 µl were withdrawn from the receiver site at 15, 30, 45, 60, 75, 90, 120, 150, 180, 210, 240, 270, 300, 330, and 360 min and replaced with blanc buffer. Additionally, samples of 40 µl were withdrawn from the donor

side in the beginning and at the end of the experiment. The samples were stored in $-20\,°C$ for later LC-MS/MS analysis. In the bevacizumab study, samples of $100\,\mu l$ were withdrawn from the receiver site at 180, 240, 270, 300, 330, 360, 390, and 420 min and replaced with blanc buffer. Samples of $10\,\mu l$ were withdrawn from the donor side in the beginning and at the end of the experiment. These samples were stored overnight in $+4\,°C$ and analyzed next day by ELISA.

The apparent permeability coefficients (P_{app}) of the eight small molecular weight drugs and bevacizumab were calculated (Eq. (1)) as:

$$P_{app,RPE-choroid}(cm/s) = J/C_0 \qquad (1)$$

where J ($ng/cm^{2}*s$) is the drug flux across the exposed membrane area ($A = 0.64\,cm^2$) in the linear range and C_0 is the initial drug concentration in the donor compartment (ng/cm^3). The sink conditions were maintained during the permeability experiments (i.e. drug concentration in the receiver side was below 10% of the donor side concentration).

2.4. Quantitative analyses

2.4.1. Small molecular drugs

The concentrations of the small molecular weight drugs in the cassette mix were analyzed with a slightly modified UPLC-MS/MS technique from previous study [12]. Minimum of eight standard curve points and blank control were used for quantitation of the compounds. Standard curve included all eight analytes and the following four deuterated internal standards: atenolol-d7, ganciclovir-d5, methotrexate-d3, and lincomycin-d3. The method was validated by including four quality control samples in three parallel sets. The linearity range varied from 1 to $1000\,ng/ml$ depending of the compound, and limit of quantitation (LOQ) was set to the lowest concentration in the standard curve for each drug. The linear concentration range for each drug is presented in Supplementary material (Table 1).

Liquid chromatography separations were carried out using Waters Acquity UPLC instrument, with the flow through needle injection system (Waters, MA, USA) coupled with Agilent Poroshell 120 SB-C18 ($2.1 \times 50\,mm$, $2.7\,\mu m$) column (Agilent Technologies, Inc., DE, USA) at $50\,°C$. The mobile phase consisted of 0.1% of formic acid in ultrapure water (A) and 100% of LC-MS grade acetonitrile (B). The gradient elution started with 2% of B at 0–1 min and continued with 2–95% of B at 1–5 min. Total run time was $9.5\,min$ including flush and equilibration of the column. The flow-rate was set to $0.3\,ml/min$ and injection volume to $0.3\,\mu l$. After every sample two wash injections, composed of a mixture of ultrapure water and isopropanol including 0.1% formic acid, were performed to prevent any carry over.

Mass spectrometry measurements were carried out using a Waters Xevo triple quadrupole mass spectrometer (TQ-S) equipped with an ESI source (Waters) operated in positive ionization mode. The optimal source parameters were: capillary voltage $3.5\,V$, cone voltage $2\,V$, source temperature $150\,°C$, desolvation temperature $500\,°C$. Nitrogen (Aga, Helsinki, Finland) was used as desolvation gas ($800\,L\,h^{-1}$) and cone gas ($150\,L\,h^{-1}$), argon (Aga, Helsinki, Finland) was used as collision gas ($0.15\,ml/min$). The multiple reaction monitoring (MRM) mode was used for quantification. The precursor and fragment ions of the small molecular weight drugs and the internal standards (with their collision energies) are presented in Supplementary material (Table 2). The resulting data was analyzed with Waters MassLynx software V4.1

2.4.2. Bevacizumab

The concentration of bevacizumab was analyzed with a BioSim™ Bevacizumab (Avastin®) (Human) ELISA Kit (E4373-100, BioVision, CA, USA) using manufacturer's protocol. The standards were prepared in BSS Plus (10 mM Hepes) buffer. The reliability of the method was checked by preparing standards also to the manufacturer's Assay Buffer.

Stability of bevacizumab was analyzed in different conditions for 6 h to assure protein stability in the permeability studies (Table 2).

Stability of bevacizumab was analyze with ELISA assays.

2.5. Calculation of RPE clearance

Contribution of RPE as elimination route from the vitreous or as a distribution route from the systemic blood circulation was estimated by calculating clearance via RPE (CL_{RPE}; ml/h) (Eqs. (2) and (3)):

$$\text{outward } CL_{RPE} = \text{outward } P_{app,RPE-choroid} \times S_{RPE} \quad \text{vitreous-to-choroid} \qquad (2)$$

$$\text{inward } CL_{RPE} = \text{inward } P_{app,RPE-choroid} \times S_{RPE} \quad \text{choroid-to-vitreous} \qquad (3)$$

where $P_{app, RPE}$ is the drug permeability (cm/s) in the RPE-choroid and S_{RPE} is the surface area of the rabbit RPE ($5.2\,cm^2$) [13].

2.6. Simulations on ocular drug entry through the RPE

The simulations were performed using the modified model from Vellonen et al. [10] (Fig. 1). In the model drug transfer between systemic blood circulation and vitreal cavity was assumed to be dictated by the distribution clearance between the blood circulation and eye (CL_{BV}). The clearance for drug elimination from the vitreous (CL_{IVT}) for ciprofloxacin, fluconazole and methotrexate were obtained from in vivo rabbit studies as calculated in del Amo et al. [5]. The CL_{BV} was obtained (1) by assuming drug entry only via the RPE using inward CL_{RPE} (Eq. (3)) or (2) by assuming all routes of entry (CL_{IVT}) into the vitreous. The drug may enter the vitreous from the systemic blood circulation across the BRB and BAB. Intravitreal drug concentrations were simulated for ciprofloxacin, methotrexate, and fluconazole using RPE entry or total entry scenarios. Only free drug was assumed to permeate across the blood ocular barriers. The fractions of free drug and protein bound drug in the plasma and vitreous were obtained from the literature [10,14]. A more detailed structure of the model, including equations and model parameters can be found from Supplementary material (Fig. 1 and Table 3).

3. Results

3.1. Drug permeability

Overall drug permeabilities in the ex vivo RPE-choroid experiments ranged over 3 orders of magnitude (from ketorolac and voriconazole to bevacizumab) indicating that the membrane was tight and intact (Table 3). The integrity of the RPE-choroid was also confirmed at the beginning of the experiments by transepithelial resistance (TER) measurements, which was $102 \pm 55\,\Omega \times cm^2$ (n = 22).

Among small molecules the range of permeability values was 13–15 fold for outward and inward permeation, also suggesting proper barrier properties (Table 3). Hydrophilic aztreonam ($LogD_{7.4}$: -4.32) had 5-times lower permeability ($4–5 \times 10^{-6}\,cm/s$) than lipophilic voriconazole ($LogD_{7.4}$: 1.21; $20–25 \times 10^{-6}\,cm/s$). The results of quinidine are not reported, because the mass balance was incomplete. Outward and inward permeability values in the isolated bovine RPE-choroid were in the same range for 5 compounds (Table 3, Fig. 2). Ciprofloxacin and ketorolac showed preferred directionality for outward permeation (Table 3; Fig. 2).

Bevacizumab (molecular weight 149 kDa) had 100- to 200-fold lower permeability than hydrophilic small molecules (aztreonam, methotrexate) and 2000 times slower outward permeation than ketorolac. The stability experiments showed that bevacizumab was stable in the permeability studies (results in Supplementary material, Table 4).
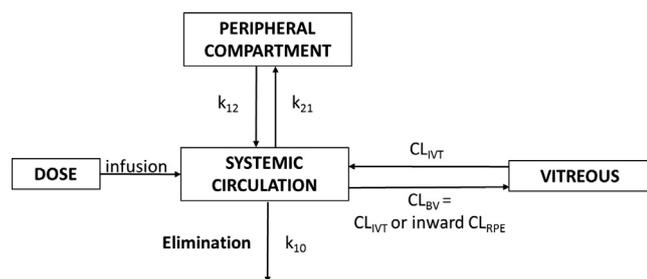
3.2. Estimated drug clearance across the RPE

The outward permeability (vitreous-to-choroid) values were used to

Table 2
Conditions of bevacizumab stability studies.

Concentration	Buffer	Temperature	Gas*	Comments
5.7 mg/ml	BSS Plus (10 mM Hepes)	37 °C	Yes	Permeability assay conditions
3 mg/ml	BSS Plus (10 mM Hepes)	37 °C	No	
3 mg/ml	BSS Plus (10 mM Hepes)	25 °C	No	
3 mg/ml	0.9% NaCl	25 °C	No	48 h stability guaranteed by the manufacturer

* 5% CO_2, 10% O_2, and 85% N_2 gas.

Fig. 1. The compartmental model used for simulating intravitreal drug concentration after systemic drug administration, adapted to the calculated inward RPE clearance values.

calculate drug clearance across the RPE-choroid (outward CL_{RPE}) (Table 4). These values were compared to *in vivo* intravitreal clearance (CL_{IVT}) values in the rabbit eye [5] (Table 4; Fig. 3). For most drugs outward CL_{RPE} values were within 2.6 fold range from CL_{IVT} values (Fig. 3, Table 4). The high outward permeability of ketorolac resulted in an outward CL_{RPE} value that was five times higher than the CL_{IVT}. Low outward permeability of bevacizumab resulted in low CL_{RPE} (about $0.035 \times CL_{IVT}$).

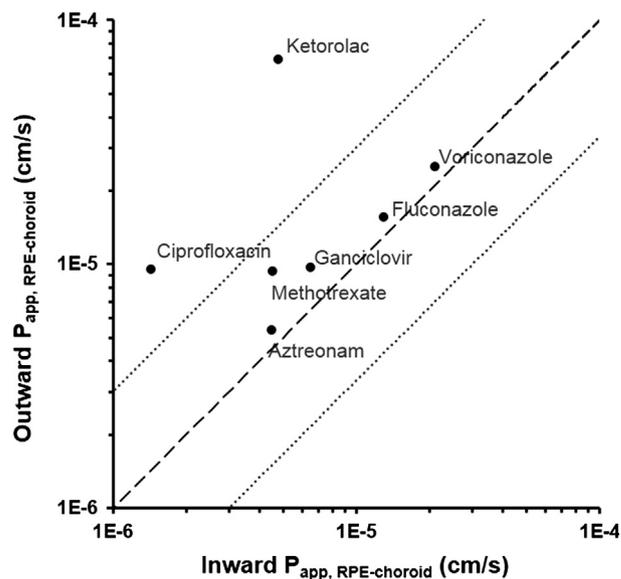### 3.3. Simulations on the RPE contribution in ocular entry of systemic drugs

Contribution of the RPE as the ocular entry route from systemic blood circulation was simulated by comparing two situations: CL_{BV} equals the inward CL_{RPE} (entry only via RPE) or CL_{IVT} (entry via all possible routes, across the BRB and BAB). In both cases, drug elimination from the vitreous was simulated using the *in vivo* intravitreal clearance (CL_{IVT}) values (including all routes of elimination) instead of the calculated outward clearance values across the RPE (outward CL_{RPE}). Table 5 shows the simulated approximate AUC values for ciprofloxacin, methotrexate, and fluconazole. The contribution of RPE as the route of entry varies among the compounds: ciprofloxacin 8%, methotrexate 43% and fluconazole 32%. Since these three compounds show higher outward than inward permeability in the RPE, it seems that in many cases the RPE has more important contribution on intravitreal drug elimination than on the drug distribution from the blood stream into the vitreous.

Fig. 2. The outward versus inward RPE-choroid permeability of the cassette dose drugs (n = 7–9). The dashed line represents identical permeabilities without directionality. The dotted lines show the situations in which inward $P_{app, \text{RPE-choroid}}$ is either 3-fold lower or 3-fold higher than outward $P_{app, \text{RPE-choroid}}$.

4. Discussion

Intravitreal injection is the most commonly used route of drug administration for the treatment of the posterior eye segment [3]. The typical range of intravitreal clearance values for small and large molecular weight compounds have been earlier defined and their routes of elimination have been proposed [5]. However, only permeability studies can give a clear insight of the route of elimination of these compounds from the vitreous. Likewise, drug entry from the blood circulation into the vitreous has been characterized and modeled [10], but the role of RPE in ocular drug entry has not been explored.

Based on the results, most of the small molecular weight drugs showed a similar outward CL_{RPE} and CL_{IVT}, which illustrates that the RPE is their main elimination route from the vitreous after intravitreal injection. Mostly the CL_{IVT} values were slightly higher than the

Table 3
Permeability data from the experiments with isolated RPE-choroid tissues.

Drug	LogD$_{7.4}$*	Molecular weight	Outward $P_{app, \text{RPE-choroid}} \times 10^{-6}$ cm/s	Inward $P_{app, \text{RPE-choroid}} \times 10^{-6}$ cm/s	Outward/Inward $P_{app, \text{RPE-choroid}}$ ratio**
Aztreonam	−4.32	435.4	5.37 ± 5.19 (n = 8)	4.47 ± 2.62 (n = 9)	1.2
Ciprofloxacin	−0.29	331.3	9.52 ± 5.28 (n = 7)	1.43 ± 0.77 (n = 8)	6.7
Fluconazole	0.45	306.3	15.64 ± 4.66 (n = 8)	12.95 ± 2.69 (n = 9)	1.2
Ganciclovir	−1.61	255.2	9.70 ± 7.90 (n = 8)	6.49 ± 3.97 (n = 9)	1.5
Ketorolac	−0.34	255.3	69.21 ± 31.9 (n = 8)	4.78 ± 3.99 (n = 9)	14.5
Methotrexate	−5.1	454.4	9.39 ± 2.74 (n = 8)	4.54 ± 2.99 (n = 8)	2.1
Voriconazole	1.21	349.3	25.00 ± 6.12 (n = 8)	21.02 ± 4.21 (n = 9)	1.2
Bevacizumab		149 000	0.035 ± 0.020 (n = 4)		

* LogD$_{7.4}$ values are computational (ACDlabs® software, version 12; Advanced Chemistry Development, Inc., Toronto, Canada).

** The outward/inward ratio is calculated based on the mean values of outward and inward $P_{app, \text{RPE-choroid}}$.

Table 4
The intravitreal clearance (CL_{IVT}) in rabbit [5] and the calculated (Eq. (2)) outward RPE-choroid clearance (CL_{RPE}) of the cassette dose drugs and bevacizumab.

Drug	CL_{IVT} (ml/h) in rabbit [5]	outward CL_{RPE} (ml/h)	CL_{IVT}/CL_{RPE}	$(CL_{RPE}/CL_{IVT}) \times 100\%$
Aztreonam	0.125	0.101 ± 0.097	1.2	81
Ciprofloxacin	0.336	0.178 ± 0.099	1.9	53
Fluconazole	0.753	0.293 ± 0.087	2.6	39
Ganciclovir	0.153	0.182 ± 0.148	0.84	119
Ketorolac	0.283	1.296 ± 0.597	0.22	458
Methotrexate	0.197	0.176 ± 0.051	1.1	89
Voriconazole	0.421	0.468 ± 0.115	0.90	111
Bevacizumab	0.019	0.000657 ± 0.000365	29	3.5
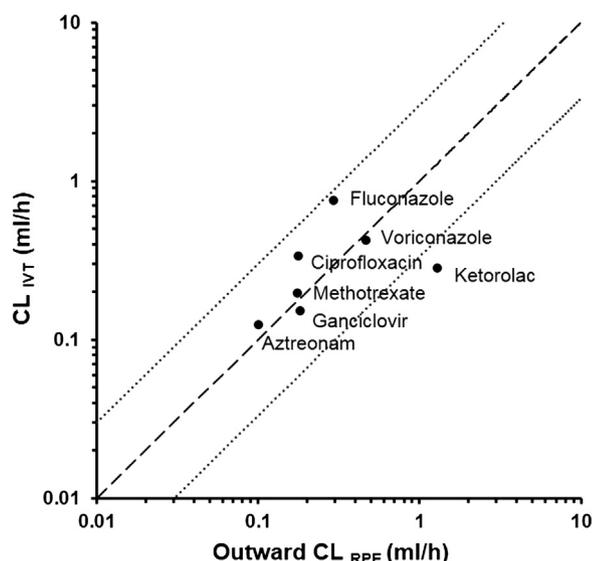
Fig. 3. Experimental intravitreal drug clearance in rabbits *in vivo* (CL_{IVT}) versus calculated outward RPE clearance (CL_{RPE}) from this study. The dashed line represents identical values for CL_{RPE} and CL_{IVT}. The dotted lines show the situations in which outward CL_{RPE} is either 3-fold lower or 3-fold higher than CL_{IVT}.

Table 5
Simulated AUC values in the vitreous after systemic delivery of ciprofloxacin 100 mg, methotrexate 12.5 mg and fluconazole 50 mg, assuming drug distribution from the blood circulation to the vitreous (CL_{BV}) equal to inward CL_{RPE} (1) or equal to CL_{IVT} (2).

Ocular entry route	CL_{BV}	AUC ($\mu g \times h/ml$) in vitreous		
		Ciprofloxacin	Methotrexate	Fluconazole
1. Only RPE	Inward CL_{RPE}*	1.56	15.89	19.85
2. All routes	CL_{IVT}	19.60	36.85	61.65

* Inward CL_{RPE} values for ciprofloxacin (0.0268 ml/h), methotrexate (0.0850 ml/h) and, fluconazole (0.242 ml/h) were based on the experimental values. Inward CL_{RPE} values were based on Eq. (3): inward CL_{RPE} = inward $P_{app,\ RPE\text{-}choroid} \times S_{RPE}$.

calculated outward CL_{RPE} values. This is most probably due to the presence of other elimination routes *in vivo*, such as aqueous humor outflow, ciliary body, and iris. On the contrary, the outward CL_{RPE} for bevacizumab (149 kDa) was only 3.5% of its intravitreal clearance, which is in line with the conclusions drawn by del Amo et al. [3], stating that only 3–20% of macromolecules (MW 4–80 kDa) are eliminated across the RPE. Hutton-Smith et al. [24] reached similar conclusions with a three-compartment semi-mechanistic model for estimating retinal permeability (RPE and inner limiting membrane) of IgG, IgG null, Fc and Fab fragment. They concluded that 13–18% of these are eliminated across the RPE and the rest via other routes.

Rabbit is the most commonly used animal model in ocular *in vivo* pharmacokinetic studies and therefore intravitreal clearance data is mainly available from this specie. However, bovine eyes were chosen as the animal model for permeability studies due to easy isolation of the RPE-choroid from bovine eyes. The RPE was isolated together or partly with the underlying choroid, but choroid is a leaky layer (TER $\approx 9\,\Omega \times cm^2$) that does not restrict the permeation of solutes [15]. Most of the small molecular weight drugs (255–454 Da), excluding ciprofloxacin and ketorolac, showed similar permeability in outward and inward directions ($P_{app,\ RPE\text{-}choroid} = 10^{-6}$–$10^{-5}$ cm/s), which is an indication of passive permeability. Bevacizumab (149 kDa) had low outward permeability of 2–3 orders of magnitude lower (10^{-8} cm/s) than the small molecular weight drugs. To our knowledge this is the first time experimental values of RPE permeability is been presented for the therapeutic drug, bevacizumab (Avastin®). Quinidine was included in the original drug mixture, but the mass balance of quinidine was incomplete, suggesting accumulation to the cell components, such as melanosomes. The choroid and RPE are enriched in melanin, and associated with prolonged retention of quinidine in the melanosomes [16,17].

Outward $P_{app,\ RPE\text{-}choroid}$ of ciprofloxacin and ketorolac were 6 and 14 times higher than their inward permeability in the bovine RPE-choroid, respectively. The directional permeability could be explained by the presence of active transporters. RPE is known to express both influx and efflux transporters on both sides of the membrane [7,9]. Ciprofloxacin had particularly low permeability in the inward direction, compared to the other small molecular weight drugs. This might be due to binding of ciprofloxacin to efflux transporter(s) in the RPE [3,18]. For example, MRP4 is known to transport ciprofloxacin and it is present in the human RPE [7,19]. Ketorolac had much higher outward permeability than the other small molecular weight drugs, while its inward permeability was in the same range with the other drugs. This may be due to influx transporter activity on the vitreal side of the RPE. For instance OAT2 is present in human RPE [7] and it is capable of transporting ketorolac [20]. Additionally, when using a mixture of drug molecules there is a possibility for transporter related interactions. Another competing drug may interfere with the permeability of a transporter dependent drug molecule. In any case, only sparse information is available of the expression and activity of transporters in the bovine RPE [9,21]. Available data suggest that the transporters may only have a modest role in the pharmacokinetics of the RPE [9].

The role of RPE in drug distribution from the systemic blood circulation into the vitreous was simulated with a modified model of Vellonen et al. [10]. The simulations showed that the RPE permeation contributes to the vitreal drug concentrations as a route of entry, but it is not necessarily a dominating one (Table 5). This could be explained by the presence of efflux transporters at the choroidal side of the RPE that may reduce the inward permeability of the drug. On the other hand, other routes of drug entry from blood circulation, such as at the BAB the nonpigmented ciliary epithelium and fenestrated vessels in the ciliary processes, could play significant role in the inward drug permeation. The nonpigmented ciliary epithelium has similar surface area as the RPE (1.4 × difference in humans [3]). Thus, BAB may play an important role in the distribution of small molecular weight drugs, but

its pharmacokinetic role is poorly known.

The information on RPE permeability is useful in developing new ocular drugs and drug delivery systems. Information on barrier permeability will be useful in building physiologically based pharmacokinetic models and finite element models that will facilitate ocular drug development [22–25].

5. Conclusions

Bidirectional permeability studies with excised RPE-choroid specimens were carried out with small molecular weight drugs and bevacizumab. The permeability values spanned over a range of three orders of magnitude. Permeability values were further used to calculate clearance values for drug transfer across the RPE from and into the eye. It seems that the RPE is the main elimination route for small molecular weight drugs from the vitreous, and efficiently blocks permeation of macromolecules, such as bevacizumab. For systemic drugs, the RPE contribute in drug distribution to the eye, but it is not the only route.

Declaration of Competing Interest

There are no conflict of interest.

Acknowledgements

Appendix A. Supplementary material

Supplementary data to this article can be found online at https://doi.org/10.1016/j.ejpb.2019.08.008.

References

[1] K. Zhang, L. Zhang, R.N. Weinreb, Ophthalmic drug discovery: novel targets and mechanisms for retinal diseases and glaucoma, Nat. Rev. Drug Discov. 11 (7) (2012) 541–559.

[2] G.D. Novack, A.L. Robin, Ocular pharmacology, J. Clin. Pharmacol. 56 (5) (2016) 517–527.

[3] E.M. del Amo, A.-K. Rimpelä, E. Heikkinen, et al., Pharmacokinetic aspects of retinal drug delivery, Prog. Retin. Eye Res. 57 (2017).

[4] D.M. Maurice, S. Mishima, Ocular pharmacokinetics, in: M.L. Sears (Ed.), Handbook of Experimental Pharmacology/Pharmacology of the Eye, Springer-Verlag, Berlin-Heidelberg, 1984, pp. 19–116.

[5] E.M. del Amo, K.S. Vellonen, H. Kidron, A. Urtti, Intravitreal clearance and volume of distribution of compounds in rabbits: in silico prediction and pharmacokinetic simulations for drug development, Eur. J. Pharm. Biopharm. 95 (2015) 215–226.

[6] R.S. Smith, L.A. Rudt, Ocular vascular and epithelial barriers to microperoxidase, Invest. Ophthalmol. Vis. Sci. 14 (7) (1975) 556–560.

[7] L. Pelkonen, K. Sato, M. Reinisalo, et al., LC-MS/MS based quantitation of ABC and SLC transporter proteins in plasma membranes of cultured primary human retinal pigment epithelium cells and immortalized ARPE19 cell line, Mol. Pharm. 14 (3) (2017) 605–613.

[8] A. Dahlin, E. Geier, S.L. Stocker, et al., Gene expression profiling of transporters in the solute carrier and ATP-binding cassette superfamilies in human eye substructures, Mol. Pharm. 10 (2) (2013) 650–663.

[9] K.S. Vellonen, L. Hellinen, E. Mannermaa, M. Ruponen, A. Urtti, H. Kidron, Expression, activity and pharmacokinetic impact of ocular transporters, Adv. Drug Deliv. Rev. 126 (2018) 3–22.

[10] K.S. Vellonen, E.M. Soini, E.M. Del Amo, A. Urtti, Prediction of ocular drug distribution from systemic blood circulation, Mol. Pharm. 13 (9) (2016) 2906–2911.

[11] L. Pitkänen, V.P. Ranta, H. Moilanen, A. Urtti, Permeability of retinal pigment epithelium: effects of permeant molecular weight and lipophilicity, Investig. Ophthalmol. Vis. Sci. 46 (2) (2005) 641–646.

[12] E. Ramsay, M. Ruponen, T. Picardat, et al., Impact of chemical structure on conjunctival drug permeability: adopting porcine conjunctiva and cassette dosing for construction of in silico model, J. Pharm. Sci. 106 (9) (2017) 2463–2471.

[13] A. Reichenbach, M. Ziegert, J. Schnitzer, et al., Development of the rabbit retina. V. The question of "columnar units", Brain Res. Dev. Brain Res. 79 (1) (1994) 72–84.

[14] A.K. Rimpelä, S. Reunanen, M. Hagström, H. Kidron, A. Urtti, Binding of small molecule drugs to porcine vitreous humor, Mol. Pharm. 15 (6) (2018) 2174–2179.

[15] S.S. Miller, J.L. Edelman, Active ion transport pathways in the bovine retinal pigment epithelium, J. Physiol. 424 (1990) 283–300.

[16] L. Pelkonen, U. Tengvall-Unadike, M. Ruponen, et al., Melanin binding study of clinical drugs with cassette dosing and rapid equilibrium dialysis inserts, Eur. J. Pharm. Sci. 109 (May) (2017) 162–168.

[17] A.K. Rimpelä, M. Reinisalo, L. Hellinen, et al., Implications of melanin binding in ocular drug delivery, Adv. Drug Deliv. Rev. 126 (2018) 23–43.

[18] DrugBank, Ciprofloxacin, transporters, https://www.drugbank.ca/drugs/DB00537, Published 2019.

[19] I.S. Haslam, J.A. Wright, D.A. O'Reilly, D.J. Sherlock, T. Coleman, N.L. Simmons, Intestinal ciprofloxacin efflux: the role of breast cancer resistance protein (ABCG2), Drug Metab. Dispos. 39 (12) (2011) 2321–2328.

[20] S. Mathialagan, M.A. Piotrowski, D.A. Tess, B. Feng, J. Litchfield, M.V. Varma, Quantitative prediction of human renal clearance and drug-drug interactions of organic anion transporter substrates using in vitro transport data: A relative activity factor approach, Drug Metab. Dispos. 45 (4) (2017) 409–417.

[21] E. Mannermaa, K.S. Vellonen, T. Ryhänen, et al., Efflux protein expression in human retinal pigment epithelium cell lines, Pharm. Res. 26 (7) (2009) 1785–1791.

[22] Y. Zhang, H. Bazzazi, E. Lima, R. Silva, et al., Three-dimensional transport model for intravitreal and suprachoroidal drug injection, Invest Ophthalmol. Vis. Sci. 59 (12) (2018) 5266–5276.

[23] L.A. Hutton-Smith, E.A. Gaffney, H.M. Byrne, A. Caruso, P.K. Maini, N.A. Mazer, Theoretical insights into the retinal dynamics of vascular endothelial growth factor in patients treated with ranibizumab, based on an ocular pharmacokinetic/pharmacodynamic model, Mol. Pharm. 15 (7) (2018) 2770–2784.

[24] L.A. Hutton-Smith, E.A. Gaffney, H.M. Byrne, P.K. Maini, K. Gadkar, N.A. Mazer, Ocular pharmacokinetics of therapeutic antibodies given by intravitreal injection: estimation of retinal permeabilities using a 3-compartment semi-mechanistic model, Mol. Pharm. 14 (8) (2017) 2690–2696.

[25] M. Lamminsalo, E. Taskinen, T. Karvinen, et al., Extended pharmacokinetic model of the rabbit eye for intravitreal and intracameral injections of macromolecules: quantitative analysis of anterior and posterior elimination pathways, Pharm. Res. 35 (153) (2018).